LEARNING ALGORITHMS WITH NEIGHBORING INPUTS IN SELF-ORGANIZING MAPS FOR IMAGE RESTORATION

Michiharu Maeda
Department of Computer Science and Engineering, Fukuoka Institute of Technology, Fukuoka, Japan

Noritaka Shigei, Hiromi Miyajima
Graduate School of Science and Engineering, Kagoshima University, Kagoshima, Japan

Keywords: Self-organizing maps, Neighboring inputs, Image restoration, Degraded image.

Abstract: This paper presents learning algorithms with neighboring inputs in self-organizing maps for image restoration. Novel approaches are described that neighboring pixels as well as a notice pixel are prepared as an input, and a degraded image is restored according to an algorithm of self-organizing maps. The algorithm creates a map containing one unit for each pixel. Utilizing pixel values as input, image inference is conducted by self-organizing maps. An updating function with threshold according to the difference between input value and inferred value is introduced, so as not to respond to noisy input sensitively. The inference of an original image proceeds appropriately since any pixel is influenced by neighboring pixels corresponding to the neighboring setting. Experimental results are presented in order to show that our approaches are effective in quality for image restoration.

1 INTRODUCTION

Self-organizing neural networks realize the network utilizing the mechanism of the lateral inhibition among neurons with the local and topological ordering. The neighboring neurons would always respond for neighboring inputs (Grossberg, 1976; Willshaw and Malsburg, 1976). For the localized inputs obviously, the outputs react locally. Huge amounts of information are locally represented and their expressions form a configuration with topological ordering. As an application of self-organizing neural networks, there are the combinatorial optimization problem, pattern recognition, vector quantization, and clustering (Hertz et al., 1991). These are useful when there exists redundancy among input data. If there is no redundancy, it is difficult to find specific patterns or features in the data. Although a number of self-organizing models exist, they differ with respect to the field of application. For self-organizing neural networks, the ordering and the convergence of weight vectors have been mainly argued (Kohonen, 1995). The former is a topic on the formation of topology preserving map, and outputs are constructed in proportion to input characteristics (Villmann et al., 1997; Maeda et al., 2007). For instance, there is the traveling salesman problem as an application of feature maps, which is possible to obtain fine results by adopting the elastic-ring method with many weights compared to inputs (Durbin and Willshaw, 1987; Angéniol et al., 1988). The latter is an issue on the approximation of pattern vectors, and the model expresses enormous information of inputs to a few weights. It is especially an important problem for the convergence of weight vectors, and asymptotic distributions and quantitative properties for weight vectors have been mainly discussed when self-organizing neural networks are applied to vector quantization (Ritter and Schulten, 1986; Ritter and Schulten, 1988; Maeda and Miyajima, 1999; Maeda et al., 2005). For image restoration, the smoothing methods, such as the moving average filter and the median filter, have been well known as a plain and useful approach (Gonzalez and Woods, 2002). From the standpoint of distinct ground, the inference of original image has been conducted by the model of Markov random field formulated statistically, based on the concept that any pixel is affected by neighboring pixels (Geman and Geman,

Maeda M., Shigei N. and Miyajima H. (2009).
LEARNING ALGORITHMS WITH NEIGHBORING INPUTS IN SELF-ORGANIZING MAPS FOR IMAGE RESTORATION.
In *Proceedings of the International Joint Conference on Computational Intelligence*, pages 331-338
DOI: 10.5220/0002280803310338

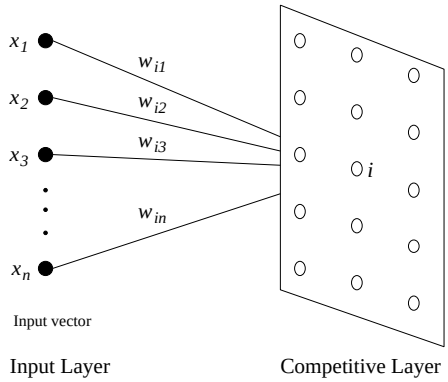

Figure 1: Structure for self-organizing maps.

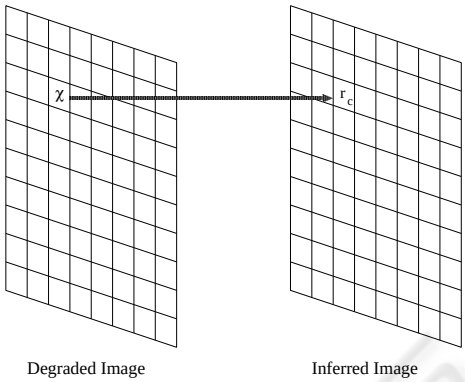

Figure 2: Correspondence between degraded image and inferred image.

1984; Maeda and Miyajima, 2004). However their algorithm require a large number of iterations since they employ the stochastic model for statistical physics.

Learning algorithms with neighboring inputs in self-organizing maps for image restoration are presented in this study. Novel approaches are described that neighboring pixels as well as a notice pixel are prepared as an input, and a degraded image is restored according to an algorithm of self-organizing maps. Our model forms a map in which one element corresponds to each pixel. Image inference is conducted by self-organizing maps using pixel values as input. A renewal function with threshold is introduced in proportion to the difference between input value and inferred value. According to this function, our approach is irresponsive to input including noise oversensitively. As any pixel is influenced by neighboring pixels corresponding to neighboring setting, the inference of an original image is appropriately promoted. Experimental results are presented in order to show that our approaches are effective in quality for image restoration.

2 SELF-ORGANIZING MAPS

Self-organizing maps realize the network with the local and topological ordering by utilizing the mechanism of the lateral inhibition among neurons. Neighboring neurons usually respond to the neighboring inputs. Huge amounts of information are locally represented and their expressions form a configuration with the topological ordering. For self-organizing maps, Kohonen's algorithm exists and is known as a popular and utility learning. In this algorithm, the updating of weights is modified to involve neighboring relations in the output array. The algorithm is applied to the structure as shown in Fig. 1. In the vector space R^n, an input x, which is generated on the probability density function $p(x)$ is defined. The input x has the components x_1 to x_n. An output unit y_i is generally arranged in an array of one- or two-dimensional maps, and is completely connected to inputs via w_{ij}.

Let $x(t)$ be an input vector at step t and let $w_i(0)$ be weight vectors at initial values in R^n space. For given input vector $x(t)$, we calculate the distance between $x(t)$ and $w_i(t)$, and select the weight vector as winner c minimizing the distance. The process is written as follows:

$$c = \arg\min_i \{\|x - w_i\|\}, \tag{1}$$

where $\arg(\cdot)$ gives the index c of the winner.

With the use of the winner c, the weight vector $w_i(t)$ is updated as follows:

$$\Delta w_i = \begin{cases} \alpha(t)(x - w_i) & (i \in N_c(t)), \\ 0 & (\text{otherwise}), \end{cases} \tag{2}$$

where $\alpha(t)$ is the learning rate and is a decreasing function of time ($0 < \alpha(t) < 1$). $N_c(t)$ has a set of indexes of topological neighborhoods for winner c at step t.

3 IMAGE RESTORATION

When self-organizing maps are adapted to the traveling salesman problem, many weights compared to inputs are used. By disposing an array of one-dimensional map for output units, fine solutions on the basis of the position of weights after learning have been obtained approximately. In the meantime, when self-organizing maps apply to vector quantization, a few weights compared to inputs are utilized for the purpose of representing huge amounts of information, and a number of discussions have been made

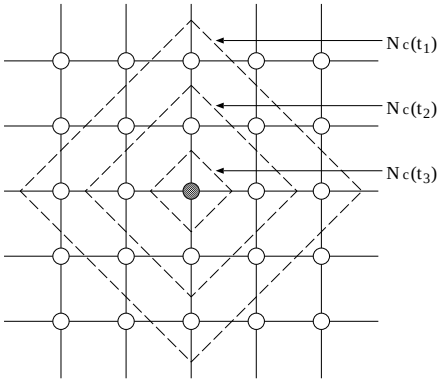

Figure 3: Distribution of topological neighborhoods.

on asymptotic distributions and quantitative properties for weight vectors.

In this section, a learning algorithm of self-organizing maps for image restoration is presented with the same number both of inputs and weights in order to infer an original image from a degraded image provided beforehand (Maeda, 2003; Maeda et al., 2008). The purpose is to infer the original image from the degraded image containing random-valued impulse noise. Here, input χ as the degraded image and weight r_i as the inferred image are defined. A map forms that one element reacts for each pixel, and image inference is executed by self-organizing maps using pixel values as input.

To begin with, the value of r_i is randomly distributed near the central value of gray scale as initial value. Next, degraded image with $l \times m$ size is given. Input χ as pixel value is arbitrarily selected in the degraded image, and let r_c be a winner of the inferred image corresponding to χ. As shown in Fig. 2, both of the positions χ and r_c agree under the degraded image and the inferred image. Therefore, inferred image r_i is updated as follows:

$$\Delta r_i = \begin{cases} \alpha(t)\Theta(\chi - r_i) & (i \in N_c(t)), \\ 0 & (\text{otherwise}), \end{cases} \tag{3}$$

where $\Theta(a)$ is a function in which the value changes with threshold $\theta(t)$ presented as follows:

$$\Theta(a) = \begin{cases} a & (|a| \leq \theta(t)), \\ 0 & (\text{otherwise}). \end{cases} \tag{4}$$

$\theta(t)$ is the difference between input χ and inferred image r_i in time t and the decreasing function of time, as $\theta(t) = \theta_0 - \lfloor \theta_0 t / T_{max} \rfloor$, where T_{max} is a maximum iteration and θ_0 is an initial threshold determined by trial and error as shown in numerical experiments. In the case of learning according to self-organizing maps, weights tend to react sensitively for noisy inputs. In order to avoid the tendency, Eq. (3) is adopted, instead of Eq. (2). By applying the function, the value which obviously differs from neighboring pixels would be disregarded. Using the functions, weights are updated until the termination condition is met. Image inference is appropriately promoted as given in the next section.

Figure 3 shows an example of the arrangement of topological neighborhoods. The circle signifies the weight and the line which connects the circles denotes the topological neighborhood. In this figure, the black circle expresses the weight of winner c. As the set of topological neighborhoods changes $N_c(t_1)$, $N_c(t_2)$, and $N_c(t_3)$ when the time varies t_1, t_2, and t_3, respectively, it is shown that the number of topological neighborhoods decreases with time. By obtaining information of the neighboring pixels, it is possible to complement lost information about pixels based on the updating function.

Image restoration by self-organizing maps (IRS) algorithm is presented as follows.

[*IRS algorithm*]

Step 1 Initialization:
Give initial weights $\{r_1(0), r_2(0), \cdots, r_{lm}(0)\}$ and maximum iteration T_{max}. $t \leftarrow 0$.

Step 2 Learning:
(2.1) Choose input χ at random among $\{\chi_1, \chi_2, \cdots, \chi_{lm}\}$.
(2.2) Select r_c corresponding to input χ.
(2.3) Update r_c and its neighborhoods according to Eq. (3).
(2.4) $t \leftarrow t+1$.

Step 3 Condition:
If $t = T_{max}$, then terminate, otherwise go to Step 2.

In this study, a peak signal to noise ratio (PSNR) P is used as the quality measure after learning for image restoration. PSNR P is presented as follows (Gersho and Gray, 1992):

$$P = 10\log_{10}(\sigma/E) \ \text{[dB]} \tag{5}$$

where σ and E are the square of gray-scale length, i.e., $\sigma = (Q-1)^2$ as a gray scale Q, and mean square error between the original image and the inferred image, respectively.

In conventional approach, one pixel of the degraded image is given as an input. In this section, novel approaches are presented that neighboring pixels as well as a notice pixel are prepared as inputs, and the degraded image is restored according to self-organizing maps. We use the following equation.

$$\Delta r_i = \begin{cases} \alpha(t)\Theta(\gamma(\chi) - r_i) & (i \in N_c(t)), \\ 0 & (\text{otherwise}), \end{cases} \tag{6}$$

Table 1: Variant models.

Model	Input
I	Average of five pixels
II	Average of nine pixels
III	Median of five pixels
IV	Median of nine pixels

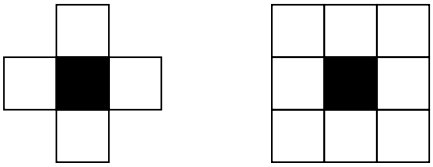

(a) Five pixels (b) Nine pixels

Figure 4: Five pixels and nine pixels used in models I, II, III, and IV.

where $\gamma(\chi)$ is a function influenced by neighboring pixels.

With respect to $\gamma(\chi)$, four models are considered as the input. Table 1 summarizes models I, II, III, and IV according to the standards of average of five pixels, average of nine pixels, median of five pixels, and median of nine pixels as the input, respectively.

In models I and III, five pixels are prepared as inputs as shown in Fig. 4 (a). Models II and IV have nine pixels as inputs (See Fig. 4 (b)). According to four models, the inputs are changed for image restoration. By altering the inputs like these, the restored images which differ in quality for the image processing are constructed as shown in the next section.

4 NUMERICAL EXPERIMENTS

In the numerical experiments, image restoration is performed to infer the original image with the size 512×512 and gray scale 256. The degraded image contains 30% noise in comparison with the original image, random-valued impulse noise, as shown in Fig. 5 (a). That is to say, the noise is included 30% pixels which are randomly chosen among the 512×512 pixels, and chosen pixels are given values from 0 to 255 at random. Initial weights are randomly distributed near the central value of gray scale Q. Parameters are chosen as follows: $l = 512$, $m = 512$, $Q = 256$, $M = 100$, $T_{max} = 100 \cdot lm$, $N(t) = N_0 - \lfloor N_0 t / T_{max} \rfloor$, and $\theta(t) = \theta_0 - \lfloor \theta_0 t / T_{max} \rfloor$.

For image restoration, Fig. 5 (b), (c), (d), (e), and (f) show results of conventional model (IRS), Model I, Model II, Model III, and Model IV, respectively. The initial neighborhood and the initial threshold are $N_0 = 3$ and $\theta_0 = 95$ for IRS, $N_0 = 6$ and $\theta_0 = 69$ for Model I, $N_0 = 7$ and $\theta_0 = 73$ for Model II, $N_0 = 3$ and $\theta_0 = 96$ for Model III, and $N_0 = 2$ and $\theta_0 = 98$ for Model IV. According to the technique given in this study, the degraded image is restorable. Model III and Model IV are better than the existing approaches.

Figure 6 shows the effect of the initial threshold θ_0 on accuracy in PSNR P for each of initial neighborhood $N_0 = 1,2,3,4,5$ for Model III and Model IV. In this case, P yields the maximum when $N_0 = 3$ and $\theta_0 = 96$ for Model III and P yields the maximum when $N_0 = 2$ and $\theta_0 = 98$ for Model IV. Figure 5 (e) and (f) were restored by these values.

As an example of another image, Fig. 7 (a) shows the degraded image. As well as the above-mentioned image, the degraded image contains the uniform noise of 30% compared to the original image. The condition of the computation is equal to that of the earlier description. According to the present algorithm, results of IRS, Model III, and Model IV are shown in Fig. 7 (b), (c), and (d), respectively. The initial neighborhood and the initial threshold are $N_0 = 3$ and $\theta_0 = 118$ for IRS, $N_0 = 7$ and $\theta_0 = 86$ for Model I, $N_0 = 7$ and $\theta_0 = 85$ for Model II, $N_0 = 2$ and $\theta_0 = 119$ for Model III, and $N_0 = 2$ and $\theta_0 = 121$ for Model IV. It is proven that the degraded image can be also restored in this case. Model III and Model IV are also greater than the existing approaches.

Figure 8 presents the effect of the initial threshold θ_0 on accuracy in PSNR P for each of initial neighborhood $N_0 = 1,2,3,4,5$ for Model III and Model IV. In this case, P yields the maximum when $N_0 = 2$ and $\theta_0 = 119$ for Model III and P yields the maximum when $N_0 = 2$ and $\theta_0 = 121$ for Model IV. Figure 7 (c) and (d) were restored by these values.

Table 2: PSNR for results of MAF, MF, IRS, Model I, Model II, Model III, and Model IV. (Unit: dB).

	Image i	Image ii
MAF	22.23	21.65
MF	29.70	28.36
IRS	30.77	28.08
Model I	24.81	23.92
Model II	24.03	23.29
Model III	31.04	29.42
Model IV	31.00	29.40

Table 2 summarizes PSNR for results of Model I, Model II, Model III, and Model IV compared to the moving average filter (MAF), the median filter (MF), and image restoration by self-organizing maps (IRS). The size of the filter mask is 3×3. It is proven that Model III and Model IV excel MAF, MF, IRS, Model I, and Model II for both images i and ii.

For Model III and Model IV, learning proceeds by

(a) Degraded image i

(b) IRS

(c) Model I

(d) Model II

(e) Model III

(f) Model IV

Figure 5: Degraded image i with 512×512 size and 256 gray-scale, and results of IRS, Model I, Model II, Model III, and Model IV.

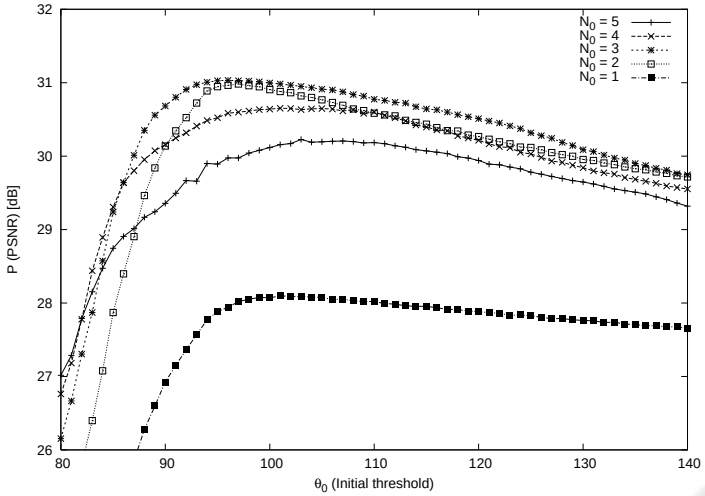

(a) Model III

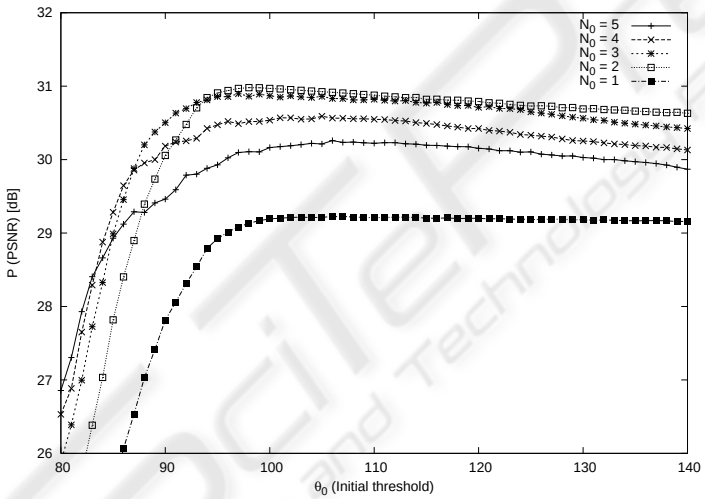

(b) Model IV

Figure 6: PSNR and initial threshold for image i.

receiving input features since neighboring pixels as well as a notice pixel are utilized. In the computational effect, Model III is faster than Model IV because object pixels of computation are four and nine for Model III and Model IV, respectively.

5 CONCLUSIONS

In this study, learning algorithms with neighboring inputs in self-organizing maps for image restoration have been presented and their validity has been shown through numerical experiments. Novel approaches were described that neighboring pixels as well as a notice pixel are prepared as an input, and a degraded image was restored according to an algorithm of self-organizing maps. Our model formed a map in which one element corresponds to each pixel. Image inference was conducted by self-organizing maps using pixel values as input. A renewal function with threshold was introduced in proportion to the difference between input value and inferred value. According to this function, our approach was irresponsive to input including noise oversensitively. As any pixel was influenced by neighboring pixels corresponding to neighboring setting, the inference of an original image was appropriately promoted. Finally, for the future works, we will study more effective techniques of our algorithms.

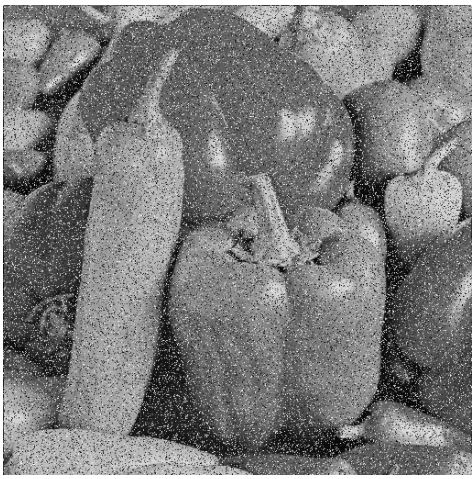

(a) Degraded image ii

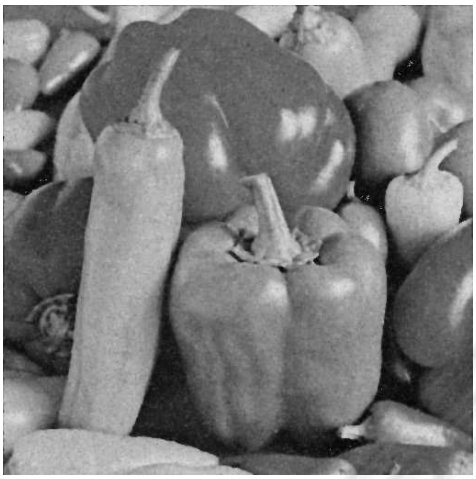

(b) IRS

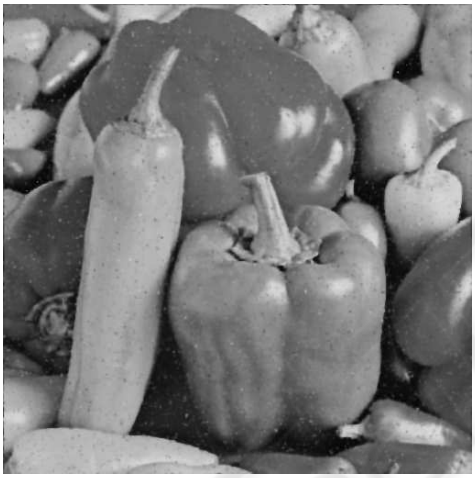

(c) Model III

(d) Model IV

Figure 7: Degraded image ii with 512×512 size and 256 gray-scale, and results of IRS, Model III, and Model IV.

REFERENCES

Angéniol, B., Vaubois, G., and Texier, J.-Y. (1988). Self-organizing feature maps and the traveling salesman problem. *Neural Networks*, 1:289–293.

Durbin, R. and Willshaw, D. (1987). An analogue approach to the traveling salesman problem using an elastic net method. *Nature*, 326:689–691.

Geman, S. and Geman, D. (1984). Stochastic relaxation, gibbs distributions, and the bayesian restoration of images. *IEEE Trans. Pattern Anal. Mach. Intel.*, 6:721–741.

Gersho, A. and Gray, R. (1992). *Vector Quantization and Signal Compression*. Kluwer Academic Publishers.

Gonzalez, R. and Woods, R. (2002). *Digital Image Processing*. Prentice Hall.

Grossberg, S. (1976). Adaptive pattern classification and universal recoding: I. parallel development and coding of neural feature detectors. *Biol. Cybern.*, 23:121–134.

Hertz, J., Krogh, A., and Palmer, R. (1991). *Introduction to the Theory of Neural Computation*. Addison-Wesley.

Kohonen, T. (1995). *Self-Organizing Maps*. Springer-Verlag Berlin.

Maeda, M. (2003). A relaxation algorithm influenced by self-organizing maps. In Kaynak, O., Alpaydin, E., Oja, E., and Xu, L., editors, *Artificial Neural Networks and Neural Information Processing*, volume LNCS2714, pages 546–553. Springer-Verlag Berlin Heidelberg.

Maeda, M. and Miyajima, H. (1999). Competitive learning methods with refractory and creative approaches. *IEICE Trans. Fundamentals*, E82–A:1825–1833.

Maeda, M. and Miyajima, H. (2004). State sharing methods in statistical fluctuation for image restoration. *IEICE Trans. Fundamentals*, E87-A:2347–2354.

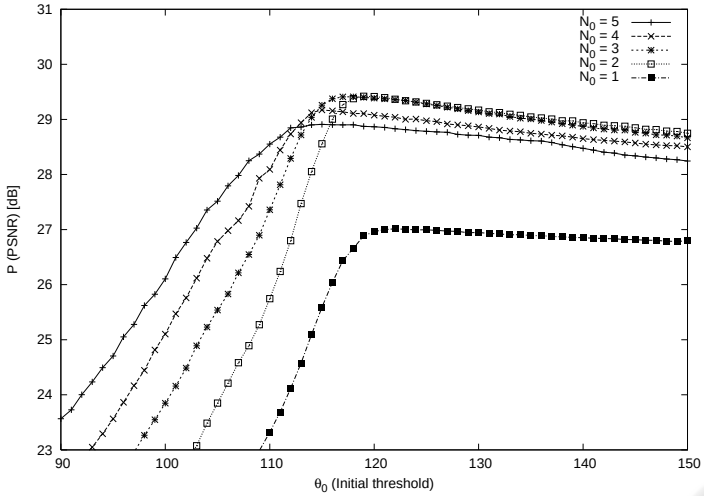

(a) Model III

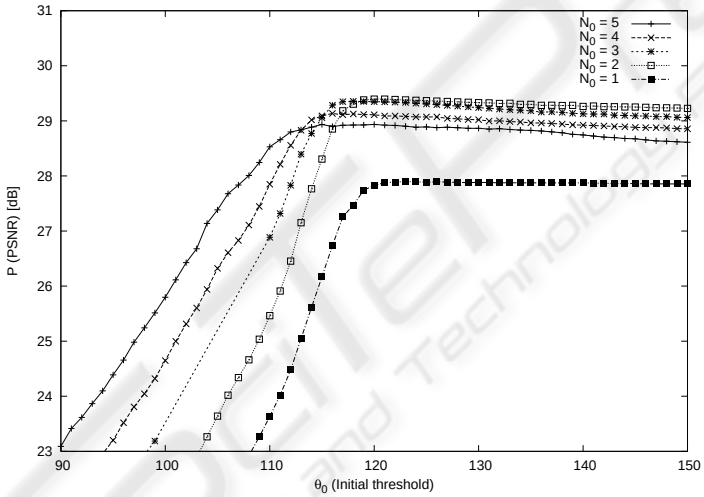

(b) Model IV

Figure 8: PSNR and initial threshold for image ii.

Maeda, M., Miyajima, H., and Shigei, N. (2007). Parallel learning model and topological measurement for self-organizing maps. *Journal of Advanced Computational Intelligence and Intelligent Informatics*, 11:327–334.

Maeda, M., Shigei, N., and Miyajima, H. (2005). Adaptive vector quantization with creation and reduction grounded in the equinumber principle. *Journal of Advanced Computational Intelligence and Intelligent Informatics*, 9:599–606.

Maeda, M., Shigei, N., and Miyajima, H. (2008). Learning model in relaxation algorithm influenced by self-organizing maps for image restoration. *IEEJ Trans. Electrical and Electronic Engineering*, 3:404–412.

Ritter, H. and Schulten, K. (1986). On the stationary state of kohonen's self-organizing sensory mapping. *Biol. Cybern.*, 54:99–106.

Ritter, H. and Schulten, K. (1988). Convergence properties of kohonen's topology conserving maps, fluctuations, stability, and dimension selection. *Biol. Cybern.*, 60:59–71.

Villmann, T., Herrmann, M., and Martinetz, T. (1997). Topology preservation in self-organizing feature maps: Exact definition and measurement. *IEEE Trans. Neural Networks*, 8:256–266.

Willshaw, D. and Malsburg, C. (1976). How patterned neural connections can be set up by self-organization. *Proc. R. Soc. Lond. B*, 194:431–445.